J. Fluid Mech. (1994), *vol.* 276, *pp.* 1–20

A theory of steady breakers

By RAYMOND COINTE† AND MARSHALL P. TULIN
Ocean Engineering Laboratory, University of California, Santa Barbara, CA 93106, USA

(Received 6 December 1991 and in revised form 17 February 1994)

The mechanics of the quasi-steady breaking wave created above a submerged hydrofoil, first studied experimentally by Duncan (1981), is elucidated here. It is an example of a flow wherein the resistance of the body manifests itself in a detached separation eddy located away from the body (i.e. on the free surface). As we show, the conditions for inception of separation and the prediction of the breaking configuration follow from simple considerations, without extensive calculation.

The physical model of the breaker, based on observations, consists of an essentially stagnant eddy riding on the forward face of the leading wave in the wave train behind the hydrofoil. This eddy is sustained by turbulent stresses acting in the shear zone separating the eddy and the underlying flow. These stresses result in a trailing turbulent wake just beneath the water surface. The breaker eddy contains air entrained at breaking, and the degree of aeration is a parameter of the problem.

The eddy–breaker model is quantified utilizing independent measurements of turbulent shear stress in shear zones. It is then shown that the hydrostatic pressure acting on the dividing streamline underneath the eddy creates a trailing wave which largely cancels the trailing wave that would exist in the absence of breaking. The 'wave' resistance of the hydrofoil then manifests itself in the momentum flux of the residual trailing wave, plus the momentum flux in the breaker wake, i.e. the breaker resistance.

For a fixed hydrofoil speed the total momentum flux, or resistance, in the presence of breaking is shown to have a minimum corresponding to a particular value of the trailing-wave steepness. It is thus concluded that the wave resistance must exceed this value for breaking to ensue. For hydrofoil resistance in excess of this minimum, both a weak and strong breaker would seem to exist. It is shown, however, that the weak breaker is unstable. It is also shown that a maximum steady breaking resistance exists, limited by the size of the breaker and dependent on the extent of its aeration.

Good quantitative comparisons between theory and experiments are shown.

1. Introduction

Under natural conditions, breaking waves are ubiquitous in the deep ocean, in the surf zone, and in the flow about ships, and they play a great role both in ocean physics and engineering. Nevertheless, our knowledge of breaking phenomena is limited. In particular, we lack basic quantitative understanding of the mechanism responsible for breaking, and of the post-breaking phase. This lack is to a great extent due to the difficulties involved in the measurement of transient phenomena, especially in the field.

A special opportunity for fundamental studies of breaking waves is presented in the case of a 'steady' spilling breaker, and this was taken advantage of by Duncan (1981, 1983) who made systematic measurements of phenomena attending the breaking of

† Present address: Mission Interministérielle de l'Effet de Serre, Ministère de l'Environnement, 20, Avenue de Ségur, 75302 Paris 07 SP, France.

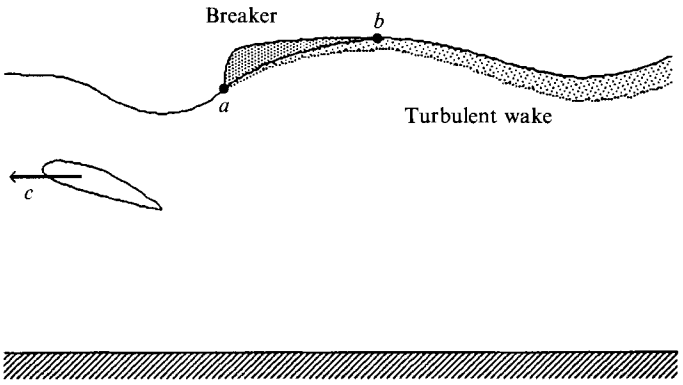

FIGURE 1. Schematic of trough, followed by a breaker sitting on the forward face and followed by a turbulent wake created along the dividing streamline *a–b*. The hydrofoil is in steady motion to the left.

waves created by towing a submerged hydrofoil in the laboratory, see figure 1. His experiments provided for the first time not only careful qualitative observations but also a set of measurements relating breaker and wave dimensions. These data raised questions and provide an opportunity for comparison with theory; they stimulated us to carry out the work reported here, which was largely completed in the theses of Cointe (1987, 1989); brief reports on the work in progress were reported in Tulin & Cointe (1986, 1987). A detailed account of the research is presented here for wider dissemination. Also, we propose a model for steady spilling breakers.

Duncan's observations give rise to a variety of questions. Some of those which have most intrigued us are: How is the onset of breaking determined in this case? Why does a fully formed breaker appear at incipient breaking? What is the relation between the hydrofoil resistance, the breaker, and the amplitude of the following waves? How does the breaker suppress the following wave?

The answers to these questions require the detailing and quantification of appropriate physical models, which began with the work of Banner & Phillips (1974). Here, after a brief review of others (§2), we describe the physical and quantitative model we have utilized (§3). The breaker is modelled explicitly as a low-energy, essentially stagnant, recirculating eddy riding on the face of the breaking wave and kept in place by the turbulent friction between the underlying flow and the eddy; the region about the boundary between this eddy and the underlying flow is modelled as a mixing zone. The breaker is trailed by a viscous momentum wake corresponding to the frictional force acting on the breaker mass. The breaker bears in this model a strong similarity to attached separated regions behind bluff bodies, as modelled by Tulin & Hsu (1980). The requirements of force equilibrium and the assumption of constant total head on the dividing streamline lead to the determination of the breaker height in terms of the crest height of the underlying wave. The resistance associated with the breaking wave is determined by two independent methods, with agreement: by a momentum balance involving a change of state between an unbroken upstream wave and the broken wave, and by direct potential wave calculation. The effect of the trailing wake is considered theoretically and shown to be small but noticeable. Some aspects of our modelling have been inspired by previous work, particularly Banner & Phillips (1974) and Duncan (1981), as discussed subsequently. However, most features of the quantification of the model and the fundamental results which follow, are believed to be wholly new.

It is shown that the existence of a steady broken wave arises from the fact that it allows the resistance acting on the foil to be balanced by the resistance of the breaker plus that of the following waves. These results tend to explain the appearance of a threshold steepness for breaking in the experiments which is not related to Stokes' limiting wave. For wave steepness beyond threshold, but below Stokes' limiting wave steepness, two breaking solutions are, in general, found to exist: a strong solution (with a large breaker) and a weak solution. Only the strong solution is found to be stable. The results are shown to be in very good qualitative and quantitative agreement with the laboratory experiments of Duncan.

It should be stressed that fundamental differences exist between transient spilling breakers at sea, and the steady spilling breakers as discussed here. Whereas the modelling developed here may be modified to deal with quasi-steady breakers coming onshore under certain circumstances, the transient behaviour of spilling breakers at sea requires the application of non-steady breaker theory.

2. Previous work

Spilling breakers as they occur at sea are transient, with effective lifetimes as short as a quarter of a wave period; an unsteady model has been proposed by Longuet-Higgins & Turner (1974), in which the breaker has been modelled as a turbulent gravity current riding down the forward face of the wave; much more remains to be done. The evidence is also mounting that the inception of breaking at sea is a consequence of non-steady wave interaction and cannot be related directly to the existence of a limiting wave, see Tulin & Li (1992); the explication of verified mechanisms awaits the future.

Somewhat more is known about 'steady' spilling breakers. They take various form in the flow around most ships, behind hydrofoils (mainly in the laboratory), in bores (or hydraulic jumps) and in quasi-steady form in the continually breaking waves on very shallow beaches. Since they can readily be produced in towing tanks and/or water channels, they provide an opportunity for detailed experimental study of breaking. They have therefore become of scientific interest despite their obvious dissimilarity to ocean transient breakers.

Spilling breakers are by their nature dissipative and at the scales which occur in nature they are turbulent in part; in addition, they are observed commonly to oscillate with a period about 4 times greater than that of the wave. They are steady, therefore, only in some mean sense.

The initial study of steady spilling breakers was made by Banner & Phillips (1974) using experiments performed by Duncan in a small flume. They gave the first qualitative description: a rolling eddy at the wave face anchored by a stagnation point at the wave crest; a turbulent wake extending behind the breaking region. Their interest was in fact in the inception of small spilling breakers, which they related to the pre-existence of a stagnation point on the wave surface. Their interest in the breaker itself was incidental and they did not therefore pursue quantitative or detailed discussion of the post-formation breaker. This work had been preceded slightly by a theoretical model of the viscous flow at the toe of the breaker, which was assumed to include a stagnation point (Longuet-Higgins 1973). This assumption had not been taken up by Banner & Phillips (1974), who found the contrary, and the origin of a mixing layer at the toe was later included in a description suggested by Peregrine & Svendsen (1978). This mixing layer plays a particular explicit role in the quantitative model of the present paper.

The Banner & Phillips (1974) initiative was continued in doctoral work by Duncan

(1981), who provided the first systemic measurements of the post-formation breaker in beautiful experiments in a small towing tank utilizing a two-dimensional submerged hydrofoil. In these experiments, conducted over a range of speeds, depths, and hydrofoil lifts, the inception of breaking was observed, the post-breaking dimensions of the breaker measured, as well as the wave face slope, the length and amplitudes of the breaking and following waves. He also surveyed the turbulent wake behind the breaking region and thereby determined the resistance associated with the breaker (Duncan 1983). The Duncan study was primarily experimental; aside from a wake momentum analysis to be used for the determination of breaker drag from experimental data, his analyses of the breaking region and of the process itself were limited to the calculation of the horizontal and vertical momentum balances for the breaking region lying above the dividing streamline, assuming a flat wave face. He thus produced the important result that the weight of the water in the breaker is supported by friction acting on the breaker face; he was thereby able to relate the breaker weight to the wake momentum deficit, and thus estimate the density of the aerated fluid in the breaker. He did not otherwise model the breaking region, or attempt to estimate the height of the breaking wave in relation to the breaker dimensions. His experimental results were startling in a number of respects and notably: (i) upon the inception of breaking, a fully formed breaker appeared; (ii) a strong repression of the following waves occurs. The current research was undertaken in response to these observations, which were not dealt with by Duncan himself.

In Duncan's picture of the flow, a large part of pressure drag on the hydrofoil, which is due to the presence of the free surface, appears as momentum loss in the turbulent surface wake. The shear stresses necessary to cause these momentum losses are created along the boundary between the overlying eddy and the flow beneath. It may be relevant to point out that this remarkable conversion of pressure drag to momentum wake also occurs in the case of the fully separated stable wake regions behind bluff bodies, where the shear stress acting on the mixing zone between the contained eddies behind the model and the outer flow accomplishes the conversion; the theory was given by Tulin & Hsu (1980).

Other and less detailed measurements of breakers behind hydrofoils were made by Battjes & Sakai (1981) and Mori (1986). The former was primarily concerned with measurements in the wake trailing the breaker, and the latter in the inception of breaking due to unstable small disturbances.

Regular surging oscillations of the 'steady' breaker were observed by Duncan (1981) at a period of 4.4 times the wave period and ascribed to resonant interaction with a specific component of the starting wave. Further observations of these oscillations were conducted by Banner (1987) in a water channel, who modelled these oscillations as a balance between the surging accelerations of the breaker mass and the resulting perturbations in shear stress along the boundary.

The present work was begun in 1985 and was largely completed in the theses of Cointe (1987, 1989).

3. Steady spilling breakers

3.1. *The model of the breaker*

Following the observations of Duncan, when the flow is steady, the breaker is regarded as a closed recirculating region of aerated water in contact with the underlying wave from the crest at point b, downward over the wave face to its leading edge or toe at point a, see figure 2. The flow is of course turbulent and exchanges take place from

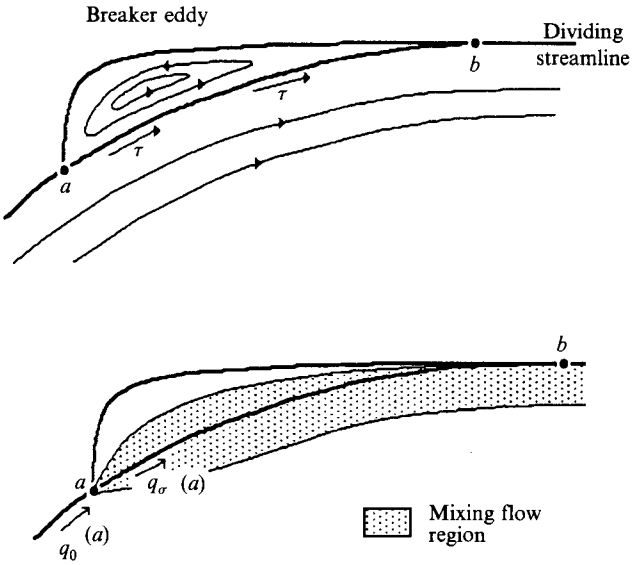

FIGURE 2. Physical model of a spilling breaker. Top: the weak eddy within the breaker, sitting on the dividing streamline *a–b* and held in place against gravity by the shear stresses τ; bottom: the region of mixing between the energetic flow below *a–b*, and the weak eddy above *a–b*, showing a discontinuity in flow speed at the eddy toe.

instant to instant between the breaker and the underlying wave, resulting in shear stresses. But we hereafter refer to the mean steady flow (i.e. time averaged) observed in a frame of reference linked with the hydrofoil.

3.1.1. *Mixing-layer model*

At the toe (*a*) the underlying flow first comes into contact with the overlying eddy. We prove subsequently, equation (10), that the dynamic pressures, and therefore the motions within the eddy, are on average at least an order of magnitude less than the hydrostatic pressures; therefore the eddy can be regarded as essentially stagnant.

The flow when a uniform stream in the lower half-space suddenly encounters stagnant fluid above was modelled in the turbulent regime by Tollmien (1926) utilizing a mixing-length model for the estimation of the shear stresses. In this model, a mixing region originates at the point (*a*) and extends in a region downstream bounded by straight lines, see figure 3. The streamline bounding the flow in the lower half-plane continues through *a*; beyond *a* this streamline divides the upper and lower mixing regions. In the upper region the stagnant flow becomes retarded. The maximum shear stress occurs on the dividing streamline and is constant along it. It rises through a discontinuity at the point *a*. As a consequence the total head and flow speed at point *a* are discontinuous and are substantially reduced upon entering the mixing zone; in Tollmien's model the speed is reduced by about half. The static pressure is essentially constant in the mixing region while the total head varies on a vertical path from its maximum value in the moving fluid to its minimum value in the stagnant region. It is a noteworthy feature of the singular flow at *a* in the Tollmien model that the finite shear stresses acting there result in a discontinuous streamwise change in the total head. The reason for this lies in the singular horizontal gradient in the shear stress at *a*. Beyond *a* on the dividing streamline, the transverse gradient in shear stress is zero (i.e. the shear stress is a maximum there), and the total head is therefore preserved constant.

The variation of total head on a dividing streamline in more complex mixing flows

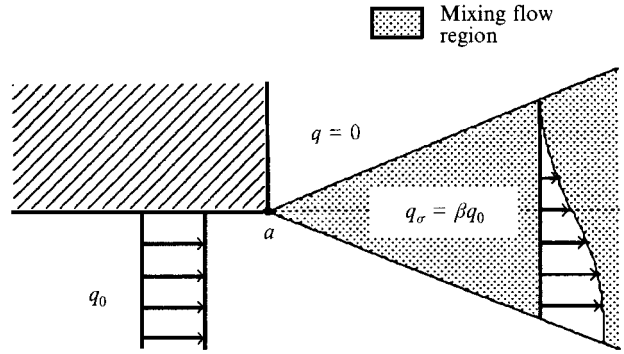

FIGURE 3. The classical turbulent-mixing-layer model, according to Tollmien (1926), where $\beta \approx 0.5$, suggesting a discontinuity in kinetic head at the toe a in the spilling breaker.

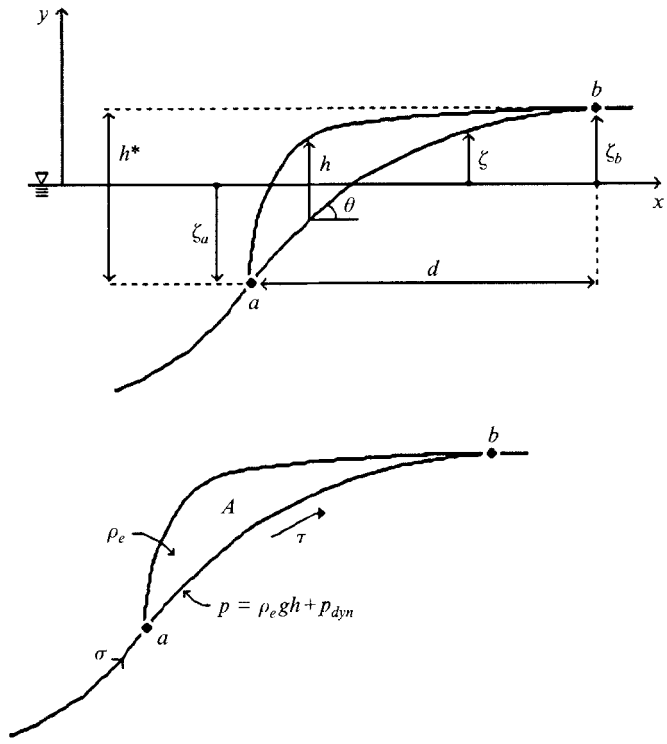

FIGURE 4. Definitions related to the steady breaker.

than the simple flow of Tollmien will again depend largely on the shear stress gradient acting there, as well as the curvature of the streamline. We resort to a past experiment, Arie & Rouse (1956), wherein a two-dimensional outer flow mixes with a stabilized, essentially stagnant, wake behind a vertical flat plate. In figure 8(*b*) of their paper, vertical profiles of total head coefficient (dark solid lines) are shown at four streamwise stations over the length of the wake. The total head, evaluated on the dividing streamline, is close to constant over the entire wake, with an average value of approximately zero. This result, obtained by detailed surveys of pressure and velocity throughout the wake, is consistent with their measurements of vertical Reynolds stress profiles, their figure 8(*c*), which are shown to peak on the dividing streamline at the first two stations, and to peak slightly below the dividing streamline at the third station.

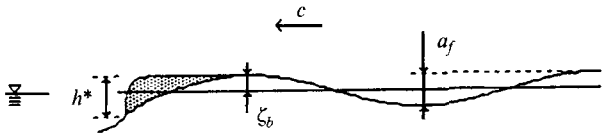

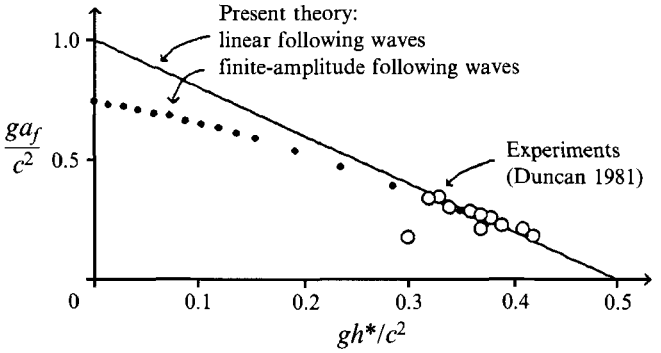

FIGURE 5. Breaker height *vs.* following wave height; present theory fitted to Duncan's (1981) data.

In view of the uniformity of total head on the dividing streamline in the mixing type of wake flow studied by Arie & Rouse we adopt the assumption of constant total head in the steady breaker flow.

We leave the jump in velocity at the toe to be determined experimentally. We write

$$q_\sigma(a) = \beta q_0(a), \tag{1}$$

where $q_0(a)$ is the flow velocity just upstream of a and $q_\sigma(a)$ is the velocity along the dividing streamline just downstream of a. Upstream of the point a, assuming no viscous effects on the approaching streamline:†

$$q_0^2(a) + 2g\zeta(a) = c^2, \tag{2}$$

where c is the velocity of the flow far upstream and $\zeta(a)$ is the free-surface elevation at point a, see figure 4. Downstream of a, the constancy of total head between a and b results in

$$q_\sigma^2(a) + 2g\zeta(a) = q_\sigma^2(b) + 2g\zeta(b), \tag{3}$$

where $\zeta(b)$ and $q_\sigma(b)$ are the elevation and the velocity at point b. Equations (1), (2) and (3) finally yield.

$$2\frac{g\zeta(b)}{c^2} = 1 - \frac{q_\sigma^2(b)}{\beta^2 c^2} - 2\frac{gh^*}{c^2}\left(\frac{1}{\beta^2} - 1\right), \tag{4}$$

where the total height of the breaker, $h^* = \zeta(b) - \zeta(a)$, has been introduced.

This result (4) is entirely consistent with Duncan's (1981) experiments, which also show that there exists a linear relationship between the height of the breaker and the height of the following waves, figure 5. When (4) is fitted to these data (assuming $2\zeta(b) = a_f$, i.e. the elevation of b relative to the mean water level is equal to half the

† The choice of Bernoulli's constant determines the position of the x-axis. In deep water, and if the wake downstream of the breaker is neglected, this x-axis coincides with the mean level (Lamb 1932).

height of the following waves; this assumption is confirmed later by potential flow computations as shown in figure 10), the slope of this relationship determines the value of β^2 (about 0.5) and its position requires that $q_\sigma(b) = 0$; i.e. that the top of the breaker is located at the crest and is a stagnation point. This both confirms the observations of Duncan and earlier of Banner & Phillips (1974), as well as the analysis made here.

Finally, we find from (4)

$$\frac{ga_f}{c^2} = 1 + \left(2 - \frac{2}{\beta^2}\right)\frac{gh^*}{c^2}. \tag{5}$$

The result, figure 5, extends Duncan's data, which involve following waves of relatively small amplitude, into the region of large-amplitude waves. Then the relationship between (4) and (5) can be modified by determining $2\zeta(b)/a_f$ from finite-amplitude (Stokes) wave theory still assuming that the elevation of b is equal to the elevation of the following crests; when this is done using numerical computations from Longuet-Higgins (1975), the dotted curve in figure 5 results.

We should emphasize that this relationship between breaker height and following wave amplitude, (5), is new and permits later analyses which lead to predictions regarding the inception of breaking. It is remarkable that this relationship follows so simply upon assumption of the constancy of total head on the dividing streamline, suggested by the mixing-layer model and the wake flow of Arie & Rouse (1956).

We may note that the largest breaker height corresponds to the case where the following wave amplitude disappears ($a_f = 0$), in which case $gh^*/c^2 = \frac{1}{2}$.

3.1.2. *Force equilibria on the steady breaker*

Important results can be obtained from force equilibria at the breaker–eddy, as shown by Duncan (1981), who found in this way that the weight of the breaker is supported by the vertical component of shear stresses acting on the dividing streamline. Here we extend his result by considering the separate contributions of hydrostatic and dynamic pressures to the force equilibria. The dynamic pressures, p_{dyn}, result from the eddying motion, and this separation allows us to show that this motion is very weak. As a result we are justified in subsequently predicting the breaker shape based on the balance between hydrostatic pressures and turbulent shear stresses acting on the dividing streamline.

The vertical equilibrium is given by (see figure 4 for nomenclature):

$$\int_a^b \int_\zeta^{\zeta+h} g \, \mathrm{d}\forall - \int_a^b p n_y \, \mathrm{d}\sigma + \int_a^b \tau n_x \, \mathrm{d}\sigma = 0, \tag{6}$$

and since the hydrostatic pressures balance gravity forces, (6) can be used to show that

$$\int_a^b p_{dyn} \, \mathrm{d}x + \int_a^b \tau \, \mathrm{d}y = 0, \tag{7}$$

where p_{dyn} is the dynamic pressure due to the circulatory motion within the eddy.

Horizontal equilibrium leads to

$$-\int_a^b p n_x \, \mathrm{d}\sigma - \int_a^b \tau n_y \, \mathrm{d}\sigma = 0, \tag{8}$$

which can also be written, introducing the hydrostatic pressure and assuming the density to be constant within the breaker,

$$\int_a^b \{(\rho_e g h + p_{dyn}) \tan\theta - \tau\} \, \mathrm{d}x = 0. \tag{9}$$

A (cm^2)	4.6	5.4	9.5	12.4	6.0	20.5	12.6	20.3	16.4	28.9	31.7	39.3
θ (deg.)	13.3	11.6	10.0	10.9	14.7	11.0	13.1	13.1	13.9	13.0	13.8	12.7
h^* (cm)	1.50	1.43	1.68	2.12	1.85	2.77	2.45	3.26	2.95	3.60	3.98	4.51
$A\sin^2\theta/4h^{*2}$	0.027	0.027	0.025	0.025	0.028	0.024	0.027	0.025	0.027	0.028	0.028	0.023

TABLE 1. Results from Duncan's (1981) experiments

An estimate of the relative importance of the dynamic pressure follows by assuming that the dividing streamline a–b is flat, constant θ. Then, eliminating τ from (7) and (9), we find

$$\left|\int_a^b p_{dyn}\,\mathrm{d}x\right| \Big/ \left|\int_a^b \rho_e g h\,\mathrm{d}x\right| = \sin^2\theta. \tag{10}$$

Duncan (1981, 1983) measured values of θ between 10° and 18° so that the dynamic pressures within the eddy are only approximately 10% of the hydrostatic pressures in magnitude, or less. This result suggests that the circulation within the eddy is negligibly weak.

Similarly, the dynamic pressure can be eliminated from (7) and (9), yielding after integration

$$\bar{\tau} d \equiv \int_a^b \tau\,\mathrm{d}x = A\rho_e g \sin\theta\cos\theta, \tag{11}$$

where d is the horizontal length of the breaker and A its area (see figure 4). This result corresponds to Duncan (1981, equation (7)).

Equations (2), (5), and (11) allow us to go beyond Duncan and to estimate the mean friction coefficient along the dividing streamline in terms of the density of the aerated breaker, ρ_e/ρ, which has not been measured:

$$c_f \equiv \frac{\bar{\tau}}{\rho q_0^2(a)} = \frac{\rho_e}{\rho}\frac{A}{4h^{*2}}\sin^2\theta. \tag{12}$$

The values measured by Duncan (1981) for the geometry of the breaker, see table 1, indicate that $A\sin^2\theta/4h^{*2}$ is constant, approximately equal to 0.026. The friction coefficient defined with $q_0(a)$ as velocity scale is therefore found to be proportional to the density ratio ρ_e/ρ:

$$c_f \approx 0.026\,(\rho_e/\rho). \tag{13}$$

This result, together with estimates of the density ratio that will be given later, yield a friction coefficient of order 0.01, a value close to that found experimentally in the mixing zone behind a bluff body (vertical flat plate) by Arie & Rouse (1956).† This is, again, an important quantitative confirmation of the mixing-layer model.

3.1.3. *Hydrostatic theory of the breaker*

The conclusion that the dynamic pressure can be neglected in comparison with the hydrostatic pressure leads to a very simple theory in which the shape of the breaker is determined by the balance between horizontal forces due to pressure and turbulent shear stresses acting on the side and bottom boundary of a vertical slice of the eddy. As a result, the height of the breaker above the dividing streamline is given by

$$\rho_e g h\frac{\mathrm{d}h}{\mathrm{d}x} = \tau - \rho_e g h\tan\theta \tag{14}$$

† From their figure 8(c), and correcting a mistake in their nomenclature, $(u'v')^{1/2}/q_\infty$ should be $u'v'/q_\infty^2$, a value of $c_f = 0.0127$ is obtained.

or
$$\rho_e g h \frac{\mathrm{d}(\zeta+h)}{\mathrm{d}x} = \tau. \tag{15}$$

Given that $\tau(a)$ is non-zero, as in the mixing layer, then in the immediate vicinity of (a), the front shape of the hydrostatic eddy is parabolic, rising rapidly as the square root of the horizontal distance from (a). Equation (15) shows moreover that the breaker height, h, has to remain smaller than $\zeta_b - \zeta_a$ as long as the shear stress remains positive. As a result, the breaker has to be inscribed in a right-angled triangle and the shape factor $h^*d/2A$ should always be greater than 1 (if θ is constant). Duncan's experiments yield values of this shape factor close to 1 and seem to show a quasi-triangular shape for the breaker. This triangular shape would correspond to the case where the shear stress is concentrated at the front of the breaker, with

$$\int_a^b \tau \,\mathrm{d}x = \tfrac{1}{2}\rho_e g h^{*2} \quad \text{or} \quad c_f = \frac{\rho_e}{\rho}\frac{\tan\theta}{8}. \tag{16}$$

The assumption that the breaker is flat-topped seems however very strong and is disputed by the observations of Banner (1987). It will therefore not be made in what follows. Actually, as will become apparent in the following analysis, an exact knowledge of the breaker shape is not necessary for the present theory; the important quantity is the integrated shear (or the value of c_f).

3.2. *The effect of the breaker on the following waves*

3.2.1. *General*

The breaker is riding on the forward face of the breaking wave and is kept in place by shear stresses acting at the dividing streamline. This determines the shape of the breaker but, reciprocally, the breaker causes a modification of the wave, comprising a strong repression of the incoming wave. This was observed and measured by Duncan but not explained and it has been one of the major goals of this theory to explain this effect quantitatively.

The breaker causes a pressure to act on the underlying wave as well as shear stresses to act on the free streamline (a)–(b), resulting in the following wake. As shown later, we can neglect the effect of the shear and its wake on the following waves for our present purpose. The pressure due to the weight of the breaker is thus primary, and it causes energy to be extracted from the underlying wave through its action. This extraction of work causes repression of the following waves. The extracted energy is dissipated in the breaker turbulence. This is the overall picture.

In the following analyses, this effect is calculated in deep water in two separate ways with agreement:

(i) by explicitly calculating the counterwave due to the breaker-induced pressure and its subtractive effect on the advancing wave;

(ii) by considering an unbroken incoming wave and by placing the breaker-induced pressure on one of the crests. The repressive effect on the following waves is then calculated by making a momentum balance across the region between unbroken and broken waves, and considering the effect of the breaker as an externally imposed force. In this balance, the wave momentum flux is, of course, a second-order quantity in wave amplitude and is known from progressive-wave theory, either linear or nonlinear. It is appropriate to think of this as a kind of shock analysis.

The shock analysis can readily be made taking nonlinear wave properties into account and these turn out to be very important. On the other hand, the counterwave

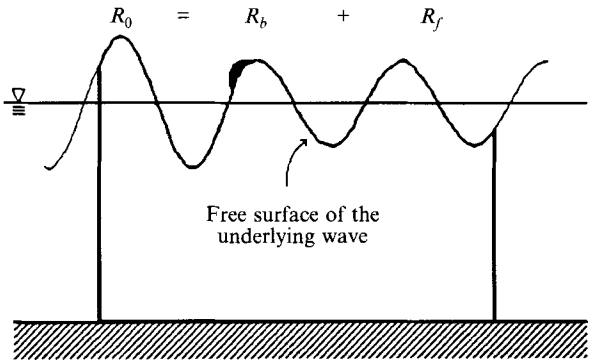

FIGURE 6. Control volume for the balance between inflowing wave momentum (R_0), resistance due to breaker (R_b), and outflowing wave momentum (R_f).

calculation is not very easy in the nonlinear regime and was not made there. Assuming linear waves, calculations made using both methods were in very good agreement. These confirm the shock analysis and at the same time prove that the wave repression is equivalent to the creation of an interfering counterwave by the breaker-induced pressures.

What is the relation between the hydrofoil flow and shock analysis? It is simply that the incoming unbroken wave is the wave that the hydrofoil would have produced in the absence of breaking. Of course, in the case of very large hydrofoil resistance, these waves could not exist as their steepness would exceed that of the Stokes limiting wave.

3.2.2. *Momentum balance: shock calculation*

The Shock Relation. We wish to calculate the repressive effect of the breaker upon the advancing wave indirectly, by applying a momentum balance. In order to perform the momentum balance, we consider the control volume shown in figure 6, which includes the free surface of the underlying wave. Note that the control volume also includes the bottom (assumed to be horizontal). Results for infinite depth are obtained by letting the depth (and, therefore, the bottom of the control volume) go to infinity. We will assume that aft of the crest b the flow is established and, therefore, periodic in x.

We first neglect the effect of shear and its wake. The breaker acts only on the breaking wave through the pressure it applies on its front face. The incoming wave momentum flux (which corresponds in Duncan's experiments to the resistance of the foil due to wavemaking) can then be written from the horizontal momentum balance as

$$R_0 = R_b + R_f, \tag{17}$$

where R_b is the resistance associated with breaking, and R_f the resistance associated with the following waves.

According to linear theory, and for infinite depth, the resistance associated with the following waves, R_f, is given by

$$R_f = \rho g a_f^2/16, \tag{18}$$

where a_f is the crest-to-trough height of the following waves. For a small value of ga_f/c^2, R_f increases therefore as the square of a_f. Integral properties of period gravity waves of finite amplitude were provided by Longuet-Higgins (1975) for infinite depth, and nonlinear effects can therefore be accounted for; the corresponding values for R_f have been tabulated (Duncan 1982; Cointe 1987) and plotted in non-dimensional form

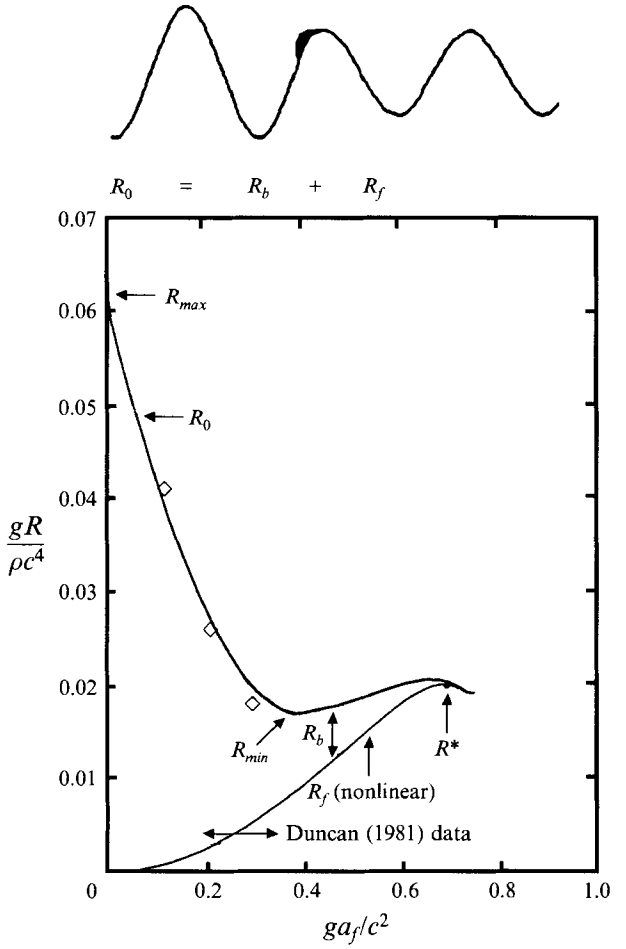

FIGURE 7. The result of the momentum (shock) analysis, R_0 *vs.* trailing wave height, a_f. Comparison with actual wave calculations, ◇, using linear theory. Also shown are the trailing wave momentum, R_f, and the breaking wave resistance.

in figure 7 as a solid line. A maximum wave resistance exists, $R^* \approx 0.02\rho c^4/g$, for a steepness slightly smaller than Stokes' limiting steepness. As a consequence, the resistance associated with a non-breaking wave train cannot exceed R^*. As a result, hydrofoil wave breaking may be regarded as a mechanism for absorbing large hydrofoil resistances.

The resistance associated with steady breaking is

$$R_b = \int_a^b p \tan\theta \, \mathrm{d}x. \tag{19}$$

If we assume a constant slope θ (but do not neglect dynamic effects within the breaker), equations (9), (11) and (12) yield

$$R_b = \int_a^b \tau \, \mathrm{d}x = 4\rho c_f g \frac{h^{*2}}{\tan\theta}. \tag{20}$$

As a result, the breaking resistance is proportional to the square of the total height of the breaker, other factors held constant. We note that both the friction coefficient

and the slope may vary somewhat with h^*. According to figure 5, h^* decreases as a_f increases. As a consequence, the breaking resistance increases as the height of the following waves decreases.

The total resistance can finally be written as

$$\frac{gR_0}{\rho c^4} = \frac{gR_f[a_f]}{\rho c^4} + \frac{\gamma}{2}\left(\frac{gh^*[a_f]}{c^2}\right)^2, \tag{21}$$

where $\gamma = 8c_f/\tan\theta$. The parameter γ is related to the mean friction coefficient or alternatively, from equation (13), to the mean density ratio, $\gamma \approx (0.208/\tan\theta)/(\rho_e/\rho)$. Actually, in the ideal case of a concentrated shear stress (equation (16)), γ is just equal to ρ_e/ρ.

In equation (21), the total resistance appears as the sum of both increasing and decreasing functions of a_f. As a consequence, R_0 can possess a minimum, R_0, for $a_f = a_{f_{min}}$. It also possesses a maximum, R_{max}, for $a_f = 0$; i.e. when the following wave train is totally suppressed. The maximum of R_f we call R^*: it corresponds to the progressive wave of maximum momentum flux. In this formulation (21), the total resistance is a function of two variables:

$$\frac{R_0}{R^*} = \frac{R_0}{R^*}\left[\frac{ga_f}{c^2}; \gamma\right] \tag{22}$$

so that a family of possible resistance relations, R_0/R^*, exists. From (5) (with $\beta^2 = 0.5$) and taking into account that linear wave properties apply well for $ga_f/c^2 < 0.4$, equation (21) reduces to

$$\frac{gR_0}{\rho c^4} \approx \frac{1}{16}\left[(1+2\gamma)\left(\frac{ga_f}{c^2}\right)^2 - 4\gamma\frac{ga_f}{c^2} + 2\gamma\right]. \tag{23}$$

Consequently, when a constant γ is assumed, it is easy to obtain

$$\frac{gR_{min}}{\rho c^4} \approx \frac{\gamma}{8(1+2\gamma)}, \tag{24}$$

$$\frac{gR_{max}}{\rho c^4} \approx \frac{\gamma}{8}. \tag{25}$$

Incipient breaking was observed by Duncan (1983) for a value of $gR/\rho c^4$ equal to 0.0166. Duncan also measured total resistances as high as $gR/\rho c^4$ equal to 0.0620 and observed that at this point the drag associated with the following wave train was almost zero. Taking these values for R_{min} and R_{max} leads to two different values of γ: 0.2 for incipient breaking and 0.5 for very strong breaking. More experiments would be needed to get an estimate of the variation of γ (that is the mean friction coefficient or the mean density ratio) with breaker strength. Lacking more experimental results, we show in figure 7 the composite curve resulting from the assumption that γ varies linearly with the height of the breaker between these two values.

According to this result derived from momentum balance: for $R_0 < R_{min}$, no solution incorporating a breaking wave exists; for $R_{min} \leqslant R_0 \leqslant R^*$, two breaking solutions exist – a *weak solution* with a smaller breaker and larger following waves and a *strong solution* with a larger breaker and smaller following waves – concurrently with the non-breaking potential solution;† for $R^* < R_0 \leqslant R_{max}$, only the strong breaking

† This is not true in the vicinity of the wave of maximum resistance where more than one non-breaking wave and one weak breaking wave can lead to the same value of R_0.

solution is possible and the residual resistance associated with the following waves is negligible; for $R_{max} < R_0$, the present model predicts that no steady breaking solution (and, of course, no steady non-breaking solution) can exist.

Assuming for now that only strong breakers can exist, these predictions strongly resemble Duncan's (1981, 1983) observations which have shown that: breaking first occurs for a steepness less than that of the limiting wave; for a certain range of total resistance, breaking and non-breaking states are possible; at the first appearance of breaking, a fully formed breaker appears; thereafter, the breaker grows with increasing hydrofoil resistance and the height of the following waves decreases.

Static Stability Analysis. In order to confirm that only strong breakers can exist, we study the static stability of the equilibrium configurations of the breaker. For that purpose, we compute the total horizontal force F_x acting on the breaker (which is exactly zero at the equilibrium point), due to a perturbation in its upstream position, a:

$$F_x = \int_a^b (\tau - p\tan\theta)\,\mathrm{d}x. \tag{26}$$

Stability corresponds to $\partial F_x/\partial a < 0$ and it can be shown that

$$F_x = R_0(a_f) - R_0 \text{ (equilibrium)}. \tag{27}$$

F_x is therefore a function of a_f only. Assuming that

$$\frac{\partial a}{\partial a_f} \approx -\frac{1}{\tan\theta}\frac{\partial h^*}{\partial a_f} > 0$$

(see (5)), it appears that the stable branches in figure 7 are those corresponding to the total resistance decreasing when a_f increases. This confirms that only strong breakers can exist.

3.2.3. *The wake: boundary-layer analysis*

The trailing wake behind the spilling breaker seems to behave very much like the turbulent wake behind a two-dimensional body, according to the measurements of Duncan (1981) and Battjes & Sakai (1981). We will, therefore, use here arguments similar to those classical boundary-layer theory along a fully submerged body. Upon the assumption that the wake is suitably thin, its effect may be calculated by finding the outer potential flow, referred to here as the pseudoflow, corresponding to the actual physical wave. The discussion given here will only use the results of the mathematical study and focus on their physical interpretation. This analysis is closely related to that of Longuet-Higgins (1969) who investigated the effect of wind shear on wave propagation.

The displacement and momentum thicknesses of the wake. The major effect is that the pseudoflow free surface is displaced downward by a distance corresponding to the wake displacement thickness, δ_1. Von Kármán's boundary-layer momentum equation applies and can be written as

$$\frac{\mathrm{d}\delta_2}{\mathrm{d}\sigma} + \frac{1}{q_\Pi}\frac{\partial q_\Pi}{\partial \sigma}(H+2)\,\delta_2 = \frac{\tau}{\rho_w q_\Pi^2}, \tag{28}$$

where δ_2 is the momentum thickness of the boundary layer, q_Π the velocity at the free surface of the pseudoflow, H the shape factor of the wake (δ_1/δ_2), and ρ_w the density of the wake.

For the far wake, the shear stress is equal to zero and we assume that the displacement and momentum thicknesses are proportional. Equation (28) yields after integration

$$\delta_1 = (c/q_\Pi)^{H+2}\Delta, \tag{29}$$

where c is the celerity of the wave and Δ a constant (the momentum thickness where $q_\Pi = c$). As the wake flows along the wavy free streamline of the pseudoflow, the pseudoflow speed fluctuates accordingly (increased in the trough and decreased at the crest), and so, therefore, does the displacement thickness. This modulation of the boundary-layer thickness is shown schematically in figure 9.

The question arises of how to relate Δ and the shear applied along the dividing streamline below the breaker. If it is assumed that $q_\Pi \approx c$ everywhere along the free surface of the pseudoflow aft of the leading edge of the breaker, point a, equation (28) yields (we assume $H = 1$ far downstream)

$$\Delta \approx \int_a^b \frac{\tau}{\rho_w c^2} \mathrm{d}\sigma. \tag{30}$$

Equation (30) gives the classical relation between the wake momentum thickness and the integral of the shear along the boundary of the dividing streamline. Duncan (1981) postulated this relation.

Combined with our estimate of the shear along the dividing streamline, estimate (30) of the wake momentum thickness yields a relation among several experimental observables:

$$\Delta = \frac{\rho_e}{\rho_w} \sin\theta \frac{gA}{c^2}. \tag{31}$$

This relation was first given by Duncan (1981) who measured Δ using a Pitot traverse in the following wave field and otherwise measured θ and A (1981, 1983). Δ is plotted as a function of $\sin\theta gA/c^2$ in figure 8. A linear relationship appears and, according to (31), leads to an estimate of ρ_e/ρ_w of around 0.5 (0.6 if only the data of Duncan's first paper are used). As the wake can be aerated, ρ_e/ρ is probably even smaller. If this estimate appears to be rather small compared to direct experimental observations, the probable range quoted by Longuet-Higgins & Turner (1974) (ρ'/ρ between 0.7 and 1) is more relevant to the density at the dividing streamline, ρ_σ, while ρ_e represents an average value of the density over the estimated surface of the breaker.

Using (12), the wake momentum thickness can also be written as

$$\frac{g\Delta}{c^2} = \frac{\gamma}{2\cos\theta}\left(\frac{gh^*}{c^2}\right)^2 \approx \frac{\gamma}{2}\left(\frac{gh^*}{c^2}\right)^2, \tag{32}$$

where $\gamma = 8c_f/\tan\theta$ is in the range [0.2–0.5].

The effect of the wake on the wavelength of the following waves. Another effect of the boundary layer is that its weight acts upon the pseudoflow free surface causing a secondary pressure. Similarly, the curvature of the streamline of the pseudoflow induces an additional secondary pressure. Along the streamline of the pseudoflow, the pressure is therefore not constant but varies with the thickness of the boundary layer. If the pressure at the free surface of the real viscous flow is constant, equal to zero, the pressure acting along the free surface of the pseudoflow is (Cointe 1987)

$$\frac{p_\Pi}{\rho} = g\cos\theta_\Pi \delta_1 + q_\Pi \frac{\partial q_\Pi}{\partial \eta}\delta_2. \tag{33}$$

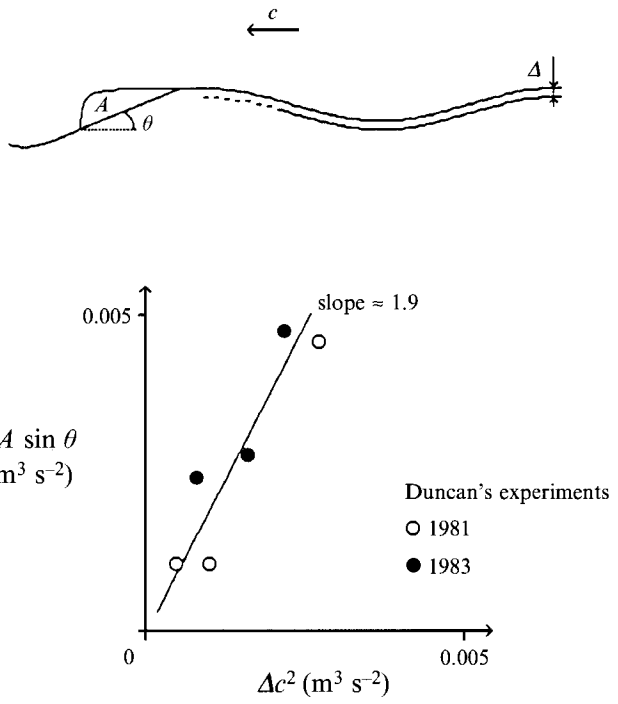

FIGURE 8. Skin friction *vs.* momentum thickness of the wake (experiments), from Duncan (1981, 1983).

For the wake aft of the crest, point b, this additional pressure causes a modification of the dispersion relation. It can be shown that the wavenumber κ corresponding to a small-amplitude wave for celerity c is (we assume $H = 1$)

$$\kappa \approx \left(1+2\frac{g\Delta}{c^2}\right)\frac{g}{c^2}. \tag{34}$$

Combining (32) and (34), we obtain finally

$$\kappa \approx \left(1+\gamma\left[\frac{gh^*}{c^2}\right]^2\right)\frac{g}{c^2}. \tag{35}$$

This relation is plotted in figure 9 for γ equal to 0.2 and 0.5. It compares rather well with Duncan's (1981) measurements of the shortened following wavelength. This effect has not been otherwise explained. In particular, the steepness of the following waves is too small for finite-amplitude effects to explain the observations since Stokes correction to the dispersion relation would give (in the absence of the wake)

$$\omega^2 = \kappa_S^2 c^2 = g\kappa_S(1+\tfrac{1}{8}a_f^2\kappa_S^2). \tag{36}$$

The corresponding correction to the linear dispersion relation is also shown in figure 9 (using (5) with $\beta^2 = 0.5$ to express a_f in terms of h^*).

The effect of the wake on the shock relation. This effect can be taken into account using an asymptotic theory (Cointe 1987) when it is assumed that both the steepness of the following waves and the thickness of the wake are small.

This analysis yields for the value of the total resistance in the presence of the wake

$$R_\Delta = R_0 - \rho g \Delta \zeta(b). \tag{37}$$

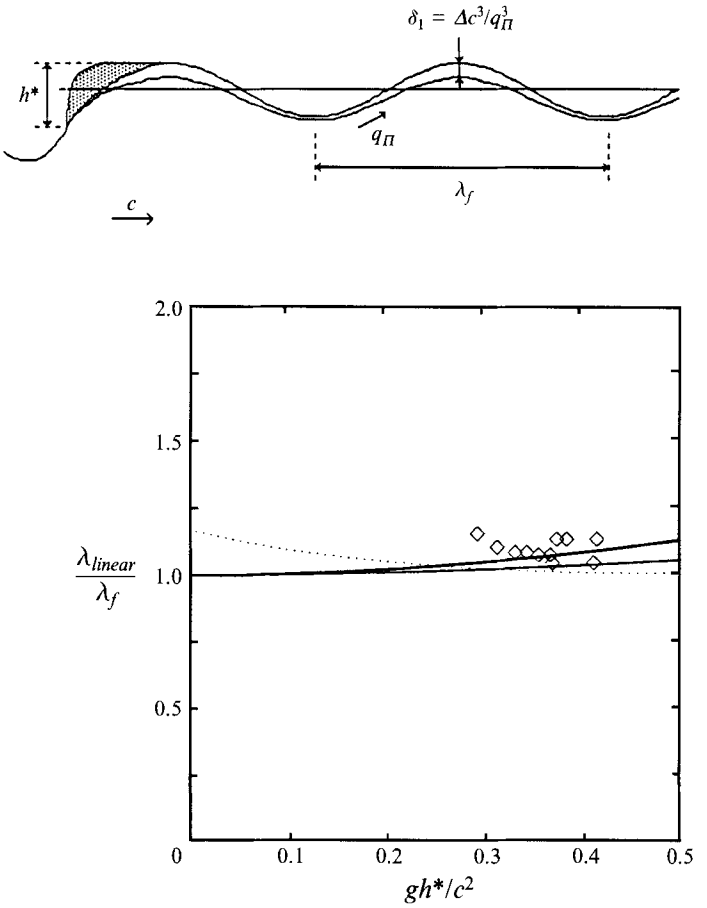

FIGURE 9. Effect of breaker wake on following wavelength: comparison of present theory *vs.* experiments. ◇, Duncan's (1981) experiments; ——, linear following waves, $\gamma = 0.2$; ——, linear following waves, $\gamma = 0.5$; · · · · · ·, Stokes correction, $\gamma = 0$.

As a consequence, the presence of the wake induces a small reduction of the minimum resistance at which breaking can occur. Note that there is no effect, at this order, of the modulation of the thickness of the wake by the orbital velocity of the wave. This result confirms that it is the pressure – and not the shear stress – which is responsible for the suppression of the following waves.

3.2.4. *Finite-depth effects*

All the preceding computations have also been carried out in finite depth. Actually, the deep-water shock relation was obtained (Cointe 1987) by considering the limit of the finite-depth result. For finite-amplitude waves, this limiting process is far from being obvious, and significant differences with Duncan's (1982) analysis are shown. Results are found to be qualitatively very similar in intermediate depth and deep water. For small-amplitude waves, the shock relations are obtained by using in (21) the corresponding expression for the wave resistance in finite depth. For finite-amplitude waves, the numerical results of Cokelet (1977) can be used.

The most interesting phenomenon which appears in finite depth is the creation of an horizontal current in the direction of wave propagation. This current is due to the wake and, therefore, is related to viscous (turbulent) phenomena accompanying breaking. It

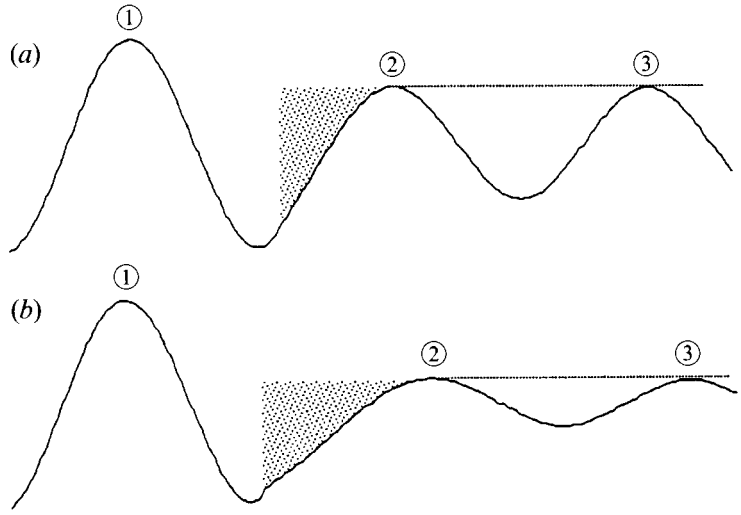

FIGURE 10. The suppressive effect on the incoming wave ① caused by a breaker (shaded) on wave ②, according to iterative numerical computations using linear theory and assuming a flat-topped breaker. Note that the crests ② and ③ have almost the same elevation. (*a*) $gR_0/\rho c^4 = 0.018$, $\gamma = 0.2$ (near incipient breaking). The vertical scale is exaggerated by a factor 9.75. (*b*) $gR_0/\rho c^4 = 0.041$, $\gamma = 0.40$. The vertical scale is exaggerated by a factor 6.5.

might be important in connection with sediment transport. The velocity of this current, c_{br}, is related to the height of the breaker, h^* (for a depth much greater than c^2/g) by

$$c_{br} \approx \frac{\gamma}{2}\frac{g}{c}\frac{h^{*2}}{D}, \tag{38}$$

where D is the water depth and c the celerity of the wave (γ is in the range [0.2–0.5]).

3.2.5. *Direct wave calculation*

The repressive effect of the breaker upon the advancing wave can also be calculated directly. Here, we take the point of view that this may be done within the framework of linear potential flow theory and we neglect the effect of the wake on the pseudoflow. As previously, in lieu of the hydrofoil wave system it is simpler to consider the more fundamental problem of a non-breaking advancing wave, height a_0, for which breaking is somehow stimulated on a particular crest, resulting in its repression and a diminished following wave. The advancing wave may be thought of as generated by a source of resistance $R_0 = \frac{1}{16}\rho g a_0^2$ (according to linear wave theory).

This computation is performed here in order to illustrate how a direct wave calculation can be done. Of course, a similar calculation could be done numerically using higher-order or fully nonlinear wave theories and/or any disturbance as the source of resistance, but with much greater computational effort.

The detailed computation using the assumptions described can be found in Cointe (1987). The main difficulty in this computation is that the pressure distribution to be applied at the free surface of the pseudoflow is not known *a priori*. For simplicity, the breaker was assumed to be flat-topped. The position of the leading edge of the breaker and the crest of the wave, as well as the height of the breaker, are found by iteration.

The computed wave profiles for a solution near incipient breaking and for a stronger breaker are shown in figure 10 for the same values of γ as in figure 7. In relation to the hydrofoil flow, the wave upstream of the breaker shown in figure 10 corresponds

closely to the wave which the hydrofoil would have produced in the absence of breaking; it cannot therefore be compared directly to the upstream wave in Duncan's (1981, 1983) experiments.

This direct numerical calculation also allows the total resistance to be related to the amplitude of the following waves; points corresponding to this calculation are shown in figure 7. The agreement between this direct counter-wave computation and the shock relation (23) is very good (for a given value of a_0 or R_0 and γ, the local geometry of the flow would be different for different shapes of the breaker but not the amplitude of the following waves) and these computations validate the assumption made in the shock calculation that the elevation of the breaking and following crests are identical. Note that, even at incipient breaking, a fully formed breaker exists.

4. Conclusions

In this paper, we have derived a physical and mathematical model for steady spilling breakers. This model, based on Duncan's (1981, 1983) observations, shows that a steady spilling breaker consists of an essentially stagnant eddy (the breaker itself) held in place on the forward face of the breaking wave by the turbulent shear stresses acting on the streamline which separates the breaker and the underlying flow.

This model leads not only a description of the geometry of the breaker but also to estimations of its effect on the breaking and following waves. Its predictions are in excellent agreement with Duncan's experiments, see figures 5, 7 and 9. The theory concludes that the existence of the broken wave arises from the fact that breaking allows the hydrofoil pressure resistance to be balanced by the breaker resistance plus that of the following wave, rather than by the following wave alone. This balance is only possible for a sufficiently large hydrofoil pressure resistance and this analysis thus explains the appearance of a threshold resistance (and therefore steepness) for steady breaking in the experiments. According to this result, breaking is therefore not a direct consequence of the existence of a Stokes' wave of limiting steepness; this result also tends to explain the existence of a marginal stability zone where both breaking and non-breaking solutions can exist.

For a resistance beyond the threshold but less than the maximum non-breaking wave resistance, two breaking regimes are, in general, found to exist: strong and weak. Only the strong regime is stable so that at threshold a fully formed strong breaker appears. For an even higher resistance, only the strong regime exists. The maximum steady breaking resistance is limited both by the size of the breaker, $gh^*/c^2 = \frac{1}{2}$, and by γ, and therefore by the friction acting between the underlying flow and the breaker. Experiments do not exist where the hydrofoil resistance exceeds this limiting resistance, so we do not know how the flow would behave in this case.

The breaker results in a wake. The displacement effect of this wake on the trailing wave results in a small increase in the wavenumber of that wave, in accord with experiments.

In shallow water, the breaker is accompanied by a horizontal current in the direction of wave propagation, equation (38), which may be of importance in connection with sediment transport.

This work has been partially supported by the Office of Naval Research Ocean Technology Program (Dr Gene Silva and Dr Steve Ramberg), and by the Institut Français du Pétrole. The authors also wish to thank Dr Mathieu Mory for pointing out a mistake in an early draft of this paper.

REFERENCES

ARIE, M. & ROUSE H. 1956 Experiments on two-dimensional flow over a normal wall. *J. Fluid Mech.* **1**, 129–141.

BANNER, M. L. 1987 Surging characteristics of spilling zones of quasi-steady breaking water waves. In *Proc. IUTAM Symp. Nonlinear Water Waves*. Springer.

BANNER, M. L. & PHILLIPS, O. M. 1974 On the incipient breaking of small scale waves. *J. Fluid Mech.* **65**, 647–656.

BATTJES, J. A. & SAKAI, T. 1981 Velocity field in a steady breaker. *J. Fluid Mech.* **111**, 421–437.

COINTE, R. 1987 A theory of breakers and breaking waves. PhD dissertation, University of California at Santa Barbara.

COINTE, R. 1989 Quelques aspects de la simulation numérique d'un canal à houle. Thèse de Doctorat, Ecole National des Ponts et Chaussées, Paris (in French).

COKELET, E. D. 1977 Steep gravity waves in water of arbitrary uniform depth. *Phil. Trans. R. Soc. Lond.* A **286**, 183–230.

DUNCAN, J. H. 1981 An experimental investigation of breaking waves produced by a towed hydrofoil. *Proc. R. Soc. Lond.* A **377**, 331–348.

DUNCAN, J. H. 1982 A note on the evaluation of the wave resistance of two-dimensional bodies from measurements of the downstream wave profile. *J. Ship Res.* **27**, 90–92.

DUNCAN, J. H. 1983 The breaking and non-breaking resistance of a two-dimensional hydrofoil. *J. Fluid Mech.* **126**, 507–520.

LAMB, H. 1932 *Hydrodynamics*. Dover.

LONGUET-HIGGINS, M. S. 1969 Action of a variable stress at the surface of water waves. *Phys. Fluids* **12**, 737–740.

LONGUET-HIGGINS, M. S. 1973 A model of flow separation at a free surface. *J. Fluid Mech.* **57**, 129–148.

LONGUET-HIGGINS, M. S. 1975 Integral properties of periodic gravity waves of finite amplitude. *Proc. R. Soc. Lond.* A **342**, 157–174.

LONGUET-HIGGINS, M. S. & TURNER, J. S. 1974 An 'entraining plume' model of a spilling breaker. *J. Fluid Mech.* **63**, 1–20.

MORI, K. 1986 Sub-breaking waves and critical conditions for their appearance. *J. Soc. Naval Archit. Japan* **159**, 1–8.

PEREGRINE, D. H. & SVENDSEN, I. A. 1978 Spilling breakers, bores and hydraulic jumps. In *Proc. 16th Coastal Engng Conf., Hamburg, Germany*, pp. 540–550.

PHILLIPS, O. M. 1985 Spectral and statistical properties of the equilibrium range in wind generated gravity waves. *J. Fluid Mech.* **156**, 505–531.

TOLLMIEN, W. 1926 Berechnung turbulenter Ausbeitungovargänge. *Z. Angew. Math. Mech.* **IV**, 468.

TULIN, M. P. & COINTE, R. 1986 A theory of spilling breakers. *Proc. 16th Symp. Naval Hydrodynamics, Berkeley*, pp. 93–105. National Academy Press, Washington, D.C.

TULIN, M. P. & COINTE, R. 1987 Steady and unsteady spilling breakers: theory. In *Proc. IUTAM Symp. Nonlinear Water Waves*. Springer.

TULIN, M. P. & HSU, C. C. 1980 New applications of cavity flow theory. In *Proc. 13th Symp. Naval Hydrodynamics, Tokyo, Japan*, pp. 107–131. National Academy Press, Washington, D.C.

TULIN, M. P. & LI, J. J. 1992 On the breaking of energetic waves. *Intl J. Offshore Polar Engng* **2**, 46–53.